EXPERIMENTAL INVESTIGATION OF THE DYNAMIC CHARACTERISTICS OF VERTICAL CLAMPED-FREE CYLINDRICAL SHELL

by

Bernardo A. Lejano

ABSTRACT

An experimental procedure was developed to investigate the dynamic characteristics of vertical clamped-free cylindrical shell. A cylindrical shell model made of rubber was constructed and tested in the dynamics laboratory of the Integrated Research and Training Center (IRTC), Technological University of the Philippines (TUP). Forced vibration tests were conducted using a shaking table while free vibration was accomplished by applying an initial displacement. The experimentally obtained dynamic characteristics show good agreement with the results using the finite element method.

INTRODUCTION

A knowledge of dynamic characteristics (i.e. natural frequencies and mode shapes) of cylindrical shell is necessary to facilitate a good design of such structure. The natural frequencies of the cylindrical shell structure must be known in order to avoid the destructive effect of resonance. The mode shapes associated with the natural frequencies are distinctly identified in terms of the circumferential mode (n) and the longitudinal mode (m). The circumferential mode pertains to the number of waves distributed around the circumference while the longitudinal mode refers to the number of waves distributed along the longitudinal axis of the cylinder. The objective of this study is to make an experimental evaluation of the dynamic characteristics of vertical clamped-free cylindrical shell. The results are compared with numerical predictions.

THE CYLINDRICAL SHELL MODEL

The cylindrical shell model was constructed out of a rectangular rubber sheet by sewing together the two edges with nylon thread and reinforcing with rugby cement. The height of the model is 45 cm, radius is 15 cm, and shell thickness is 0.45 cm. The cylinder was mounted on a plyboard base by wedging the rubber in the circular cutout made on the plyboard and applying rugby cement. Rubber was chosen to be used as material for the construction of the cylindrical shell model because of its inherent low modulus of elasticity which would lower the natural frequencies to the capacity of the instruments. Furthermore, rubber has a wide elastic range which would easily satisfy the assumptions that all deformations are linear and within the elastic region.

Five rubber strips with measurements given in Table 1 were prepared from the same rubber sheet from which the cylindrical shell model was made. Two strain gages were attached to the middle portion of each rubber strip to measure the longitudinal strain, ex, and the transverse strain, ey. The strain gages were hooked up to the TDS-301 data logger for monitoring of strains. The loading is done by clamping one end of the strip to a stationary support, and applying incremental weights on the other end. Lead shots were used as incremental loads. The total weight applied and the strains for each loading stage were carefully recorded.

The modulus of elasticity was determined by plotting the recorded longitudinal strain against the applied stresses as shown in Figure 1. The least square method was used to determine the slope of the best fit line. The average modulus of elasticity is 672.1 kg/cm^2.

Poisson's ratio is the ratio of the transverse strain against the longitudinal strain. This is shown in Figure 2. The average Possion's ratio of the rubber is 0.375.

The mass density of a material is equal to the density divided by the gravitational acceleration. To determine the density of the rubber, the weight and volume of each rubber strips were measured. Presented in Table 1 are measurements of the rubber strip samples. The average mass density of the rubber is 1.727E-6 $kg\text{-}sec^2/cm^4$.

Table 1

Measured data of the rubber strip samples

Sample No.	Length (cm)	Width (cm)	Thickness (cm)	Weight (g)	Mass Density ($kg\text{-}sec^2/cm^4$)
1	16.00	1.98	0.37	20.4	1.776E-6
2	14.92	2.09	0.44	22.9	1.703E-6
3	16.00	2.48	0.43	28.5	1.704E-6
4	16.05	2.47	0.44	29.5	1.723E-6
5	15.98	2.16	0.38	22.2	1.726E-6

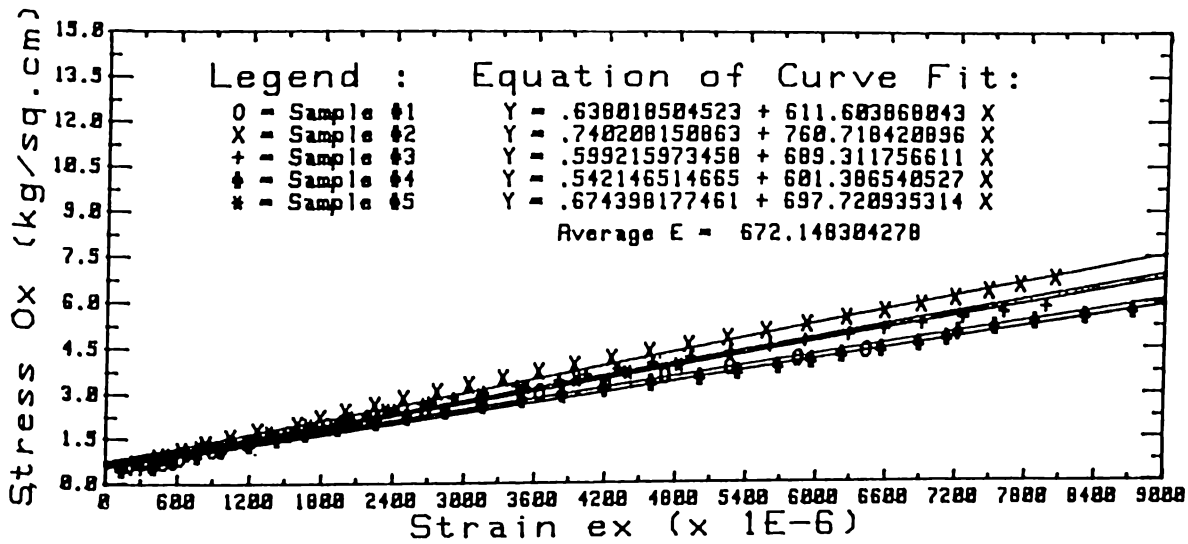

Fig. 1 - Stress-Strain curve of rubber used.

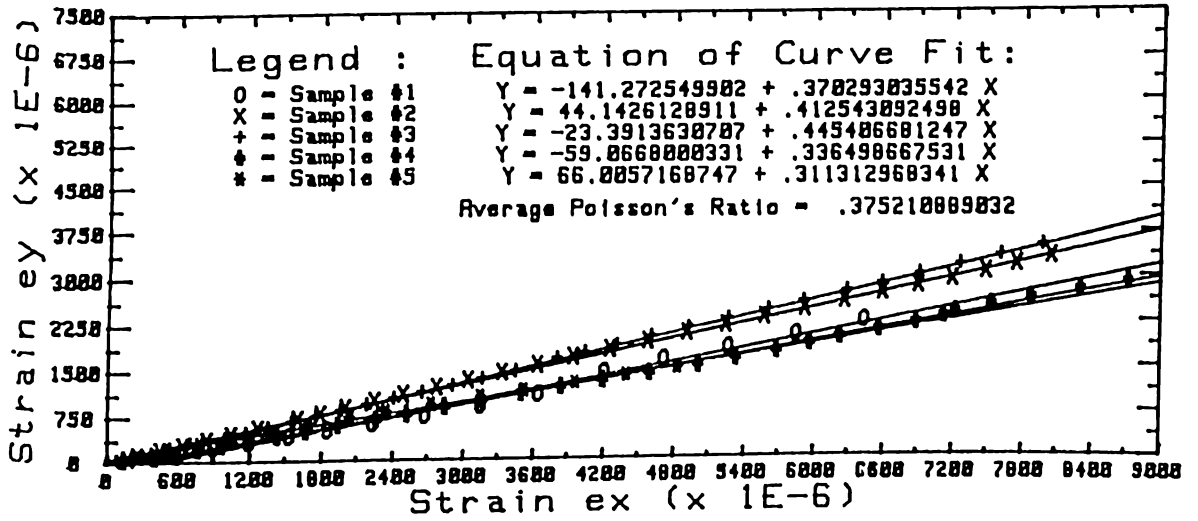

Fig. 2 - Plot of ex versus ey

CALCULATED NATURAL FREQUENCIES

Having obtained the essential properties of rubber, the natural frequencies and mode shapes were calculated using finite element method. The results are tabulated in Table 2. Due to the limitation of the capacity of the equipment, only natural frequencies below 40 Hz were experimentally investigated.

Table 2 - Calculated natural frequencies (Hertz).

Circumferential Wave No. (n)	Longitudinal Mode (m)		
	1	2	3
0	107.8642	202.6187	208.6337
1	35.5575	104.5972	158.8005
2	16.5786	62.3831	119.5851
3	17.1123	42.4766	85.5920
4	28.9610	41.1118	70.3379
5	45.9587	53.0486	71.7452

EXPERIMENT SET-UP

Two experiment set-ups were prepared, one for the forced vibration test and the other for the free vibration test. In forced vibration, the model was mounted on top of the shaking table. Vibration was induced to the model via the shaking table as if a ground induced excitation. In free vibration test, the model was given an initial displacement and the movement of the model was observed as the initial displacement was released.

A schematic diagram of the dynamic loading system for forced vibration test is shown in Fig.3. The dynamic loading is controlled with an electric-hydraulic system. The signal source unit generates sinusoidal voltage signal which is transmitted to the control panel. The control panel in turn amplifies the signal and send it to the servo-control system of the shaking table. This servo-control, which is mainly an electrically controlled valve, transforms the signal into mechanical motions by inducing the oil pressure unit to give off varying pressure corresponding to the electrical signal and thereby producing the vibratory motions of the shaking table. The shaking table used is a constant-displacement vibration machine, that is, it attempts to maintain constant displacement amplitude while the frequency is varied.

The vibration of the model was monitored and recorded using the measurement system depicted in Figure 4. The strain gages, acceleration meter, and displacement transducers measure strain, acceleration, and displacement, respectively, in terms of change in electrical resistance. The dynamic strain amplifier amplifies these changes in electrical resistance and output these in terms of voltage signals. These voltage signals are converted into digital data using the AD (Analog to Digital) converter which is interfaced with the NEC-PC 9801 personal computer. The digitized data are then stored in a floppy disk for data analysis. Computer programs were written to control the data sampling process.

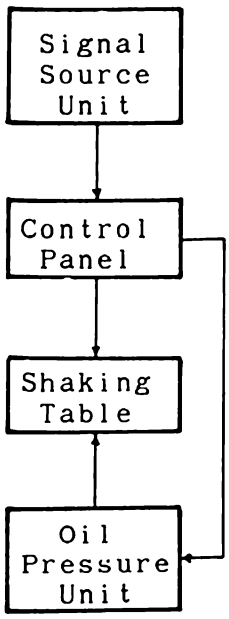

Fig.3 - Loading System

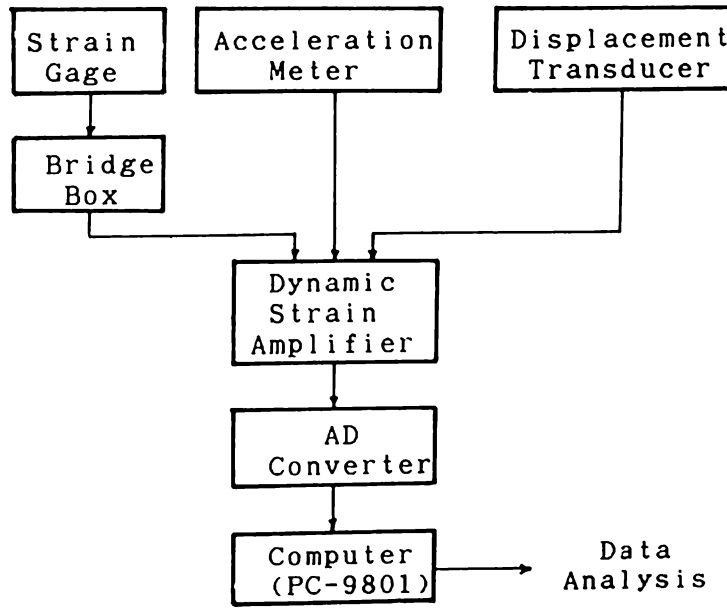

Fig.4 - Measurement System

To convert the voltage signal generated by the sensors into the corresponding unit of measurement, each sensor has to be calibrated. The calibration factor is obtained by determining the ratio of electrical output to the analog input. The acceleration meter was calibrated using earth's gravitational field. A 2g change in acceleration may be obtained by first orienting the acceleration meter with the positive direction of its sensing axis up, and then rotating the acceleration meter through 180 ^{o} so that the positive direction is down. For the strain gages, the manufacturer has supplied the calibration factor. The displacement transducer was calibrated by giving several known displacements (measured using caliper) and measuring the corresponding voltage output.

A total of 18 measuring points were established. However only eight sensors were used at a time because only eight monitoring channels are available. Location of sensors on the model is shown in Figure 5.

FREQUENCY SWEEPER TEST

Resonance occurs when a structure is subjected to a dynamic load having frequency equal to the natural frequency of the structure. This is the principle used to identify experimentally the natural frequencies of the cylindrical shell model. The frequency sweeper is a forced vibration test in which the shaking table is vibrated following a sine wave input signal of varying frequencies at a specified span of time. The response of the model is monitored to pinpoint the frequencies corresponding the maximum deformations.

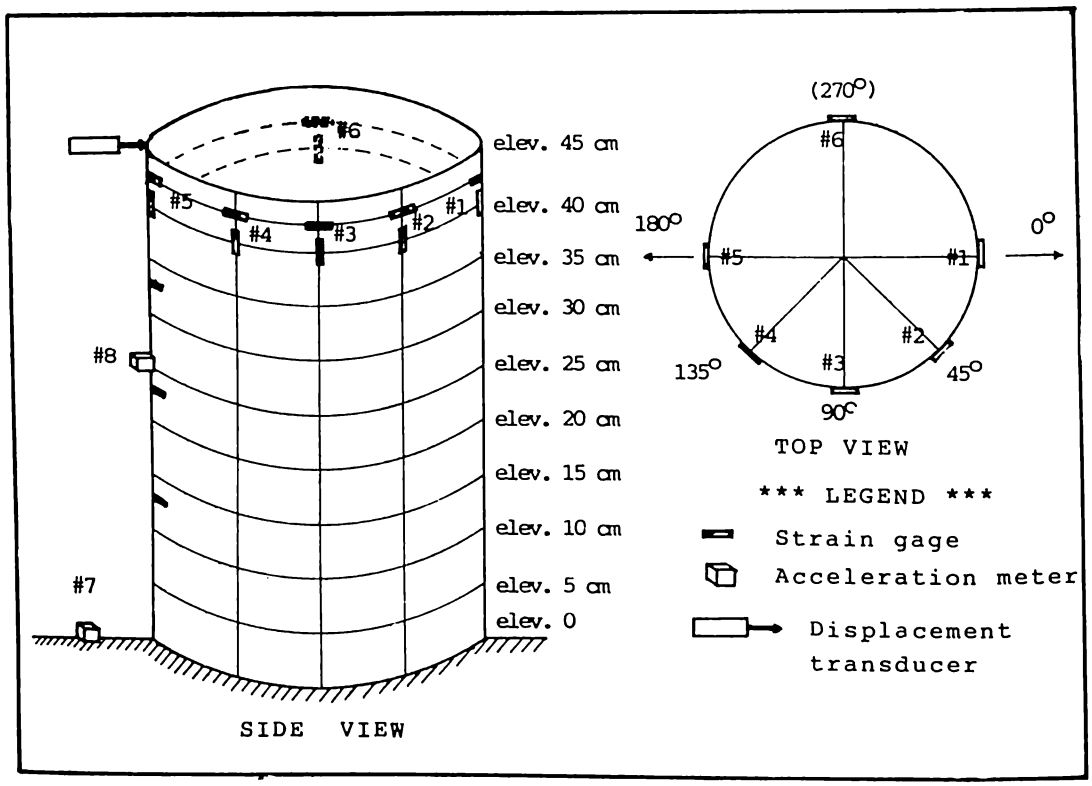

Fig. 5 - Location of sensors on the cylindrical shell model.

The frequency range used was 0-40 Hz at a span of 20.48 seconds. This means that the starting frequency was 0 Hz at time = 0 and the frequency was increased uniformly until 40 Hz was attained at time = 20.48 sec. The measurements were done for the circumferential strains at elevation 42.5 cm., and for the longitudinal strains at elevation 40 cm. The response acceleration of the model at elevation 25 cm along the line of action of the shaking table was monitored using channel 8. The data sampling interval used was 10 millisecond.

Presented in Figure 6 is the time history response of the model measured via the circumferential strain. It is clearly seen in the graph that responses become very large at certain stages of the frequency sweep. These are when resonance occur. To emphasize the frequencies at which resonance occur, spectral analysis was performed using the Fast Fourier Transform (FFT). The spectra from the time history response are shown in Figure 7. A summary of the frequencies corresponding to the observed peaks in the spectra is presented in Table 3. The average measured natural frequencies is presented in Table 4. The comparison between the computed natural frequencies and those obtained from experiment shows that there is a good agreement between the two.

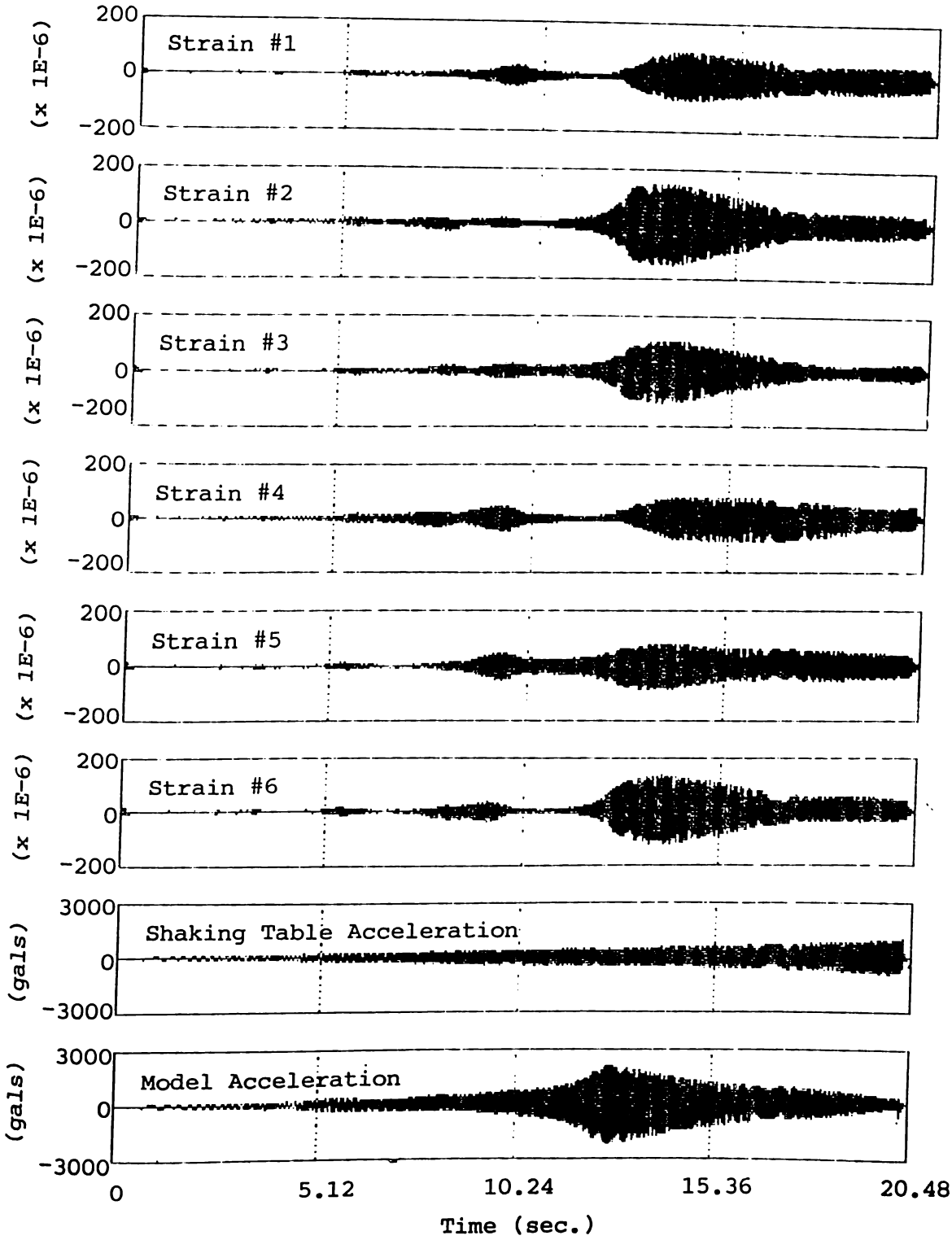

Fig. 6 - Time history response (circumferential strain) due to frequency sweeper of range 0-40 Hz.

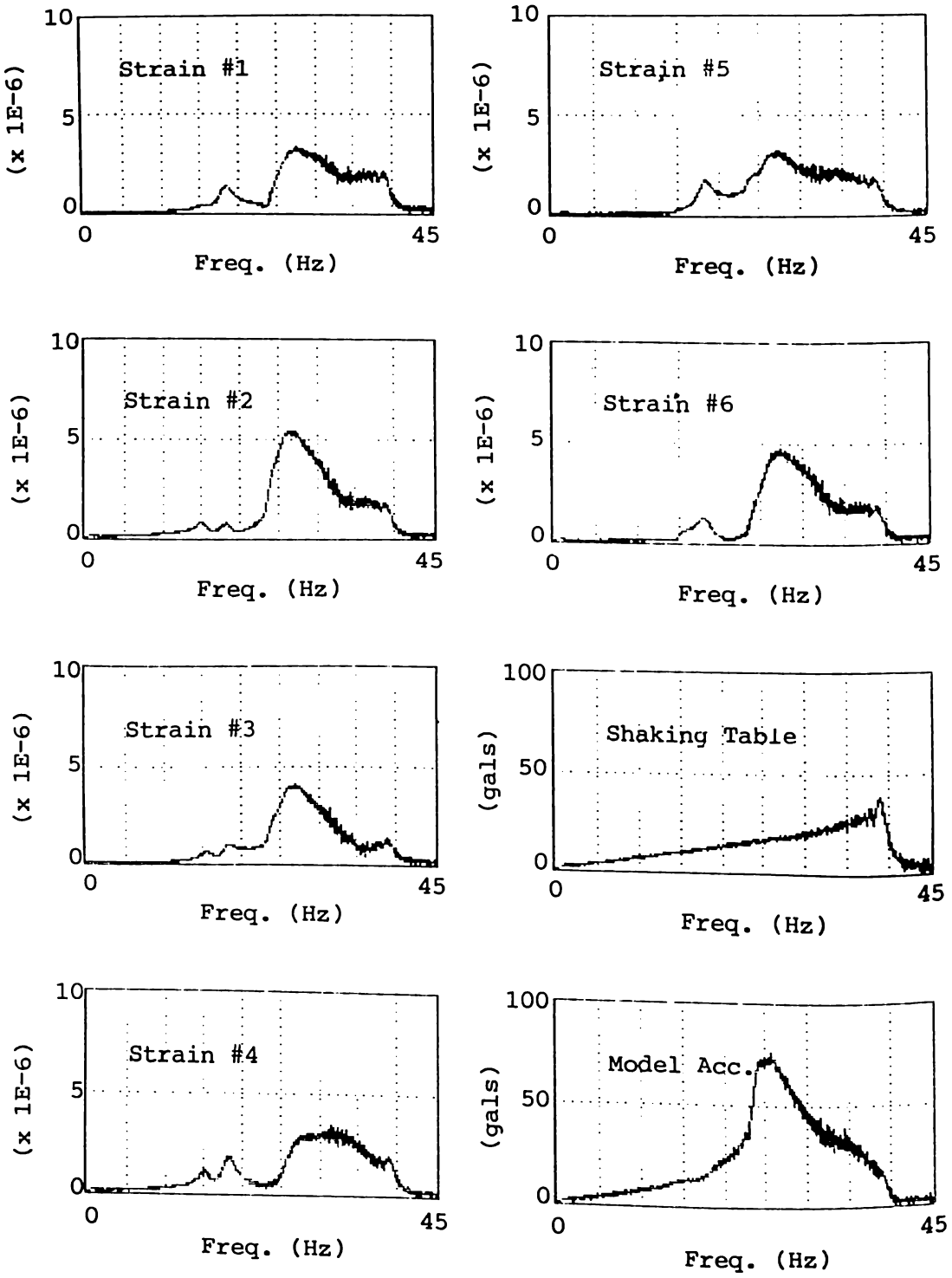

Fig. 7 - Spectra of frequency sweeper test results.
(sweeper range : 0 - 40 Hz)

Table 3 - Natural frequency (Hz) from frequency sweeper test.

Chan.#	Circumferential strain			Longitudinal Strain		
	Peak 1	Peak 2	Peak 3	Peak 1	Peak 2	Peak 3
1	15.723	18.457	27.441	****	****	27.344
2	15.004	18.262	26.562	15.186	18.018	26.416
3	15.527	18.261	27.002	15.527	18.164	26.416
4	15.137	18.262	****	15.235	18.018	****
5	****	18.457	27.051	15.186	19.287	26.416
6	15.820	17.969	27.246	15.674	18.115	26.562
8	****	****	25.586	****	****	24.805

Note : **** - Frequency not distinct in the spectrum.

Table 4 - Comparison between frequency sweeper result and calculated natural frequencies.

FEM results	16.579 Hz	17.112 Hz	28.961 Hz
Freq. Sweeper	15.342 Hz	18.297 Hz	26.570 Hz
Ratio (Calc/Expt)	1.076	0.935	1.090
Percent Difference	7.6 %	-6.5 %	9.0 %

STEADY-STATE VIBRATION TEST

Steady-state vibration test was coined by the author referring to the sampling of the steady-state response of the model as the shaking table was vibrated sinusoidally to a designated frequency. The frequency of the sine wave, used as input signal to the shaking table, was changed for each sampling. The sampling was started from 10 Hz, incrementing the applied frequency by one hertz for each sampling until 40 Hz was reached. The amplitude of the shaking table's acceleration was fixed to 600 gals. The sampling time used was 0.256 sec with a sampling interval of 1 millisecond. The amplitude of each sampled steady-state response was measured to establish an amplitude-frequency graph. Presented in Figure 8 is the resulting amplitude-frequency graph. The strain amplitudes peaked at 14 Hz, 18 Hz, and between 23-29 Hz (with more peaks occuring at 26 Hz). This indicates good agreement with those obtained from the frequency sweeper test.

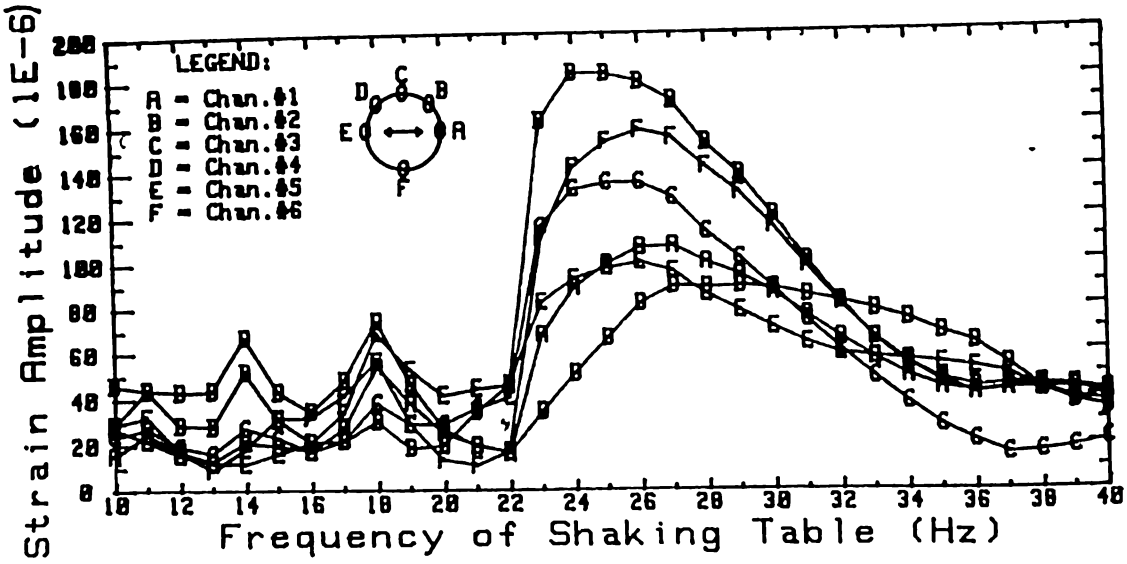

Fig. 8 - Amplitude-frequency graph

In order to know if the experimentally obtained natural frequencies really matched those of the calculated ones, the governing circumferential deformation shape is drawn from the sampled steady state response data. The radial displacements, w, at points where the strain gages were placed were approximated from the circumferential strain, ε_t, as

$$w = r\,\varepsilon_t$$

where r is the radius. Presented in Figure 9 are the experimentally obtained circumferential deformation shapes during vibration. It may be concluded that the experimentally obtained natural frequencies matched those of numerically obtained.

The longitudinal mode shapes were also verified by monitoring the circumferential strains at elevations 12.5, 22.5, 32.5, and 42.5 cm at $\theta = 180^{o}$ as depicted in the positions of strain gages in Figure 5. The deformation shapes were obtained by performing steady-state vibration test for frequencies near resonance. The result is shown in Figure 10. It is observed that the axial mode shape m = 1 is very distinct at frequency where peaks were observed.

FREE VIBRATION TEST

The sudden release of an initial displacement applied on the model produces free vibration. A point load is applied at the top of the model at $\theta = 0$ to cause an initial displacement. This is done by attaching a piece of string at the upper edge of the model and pulling it outward to produce a 2 cm displacement at the point where the string was attached.

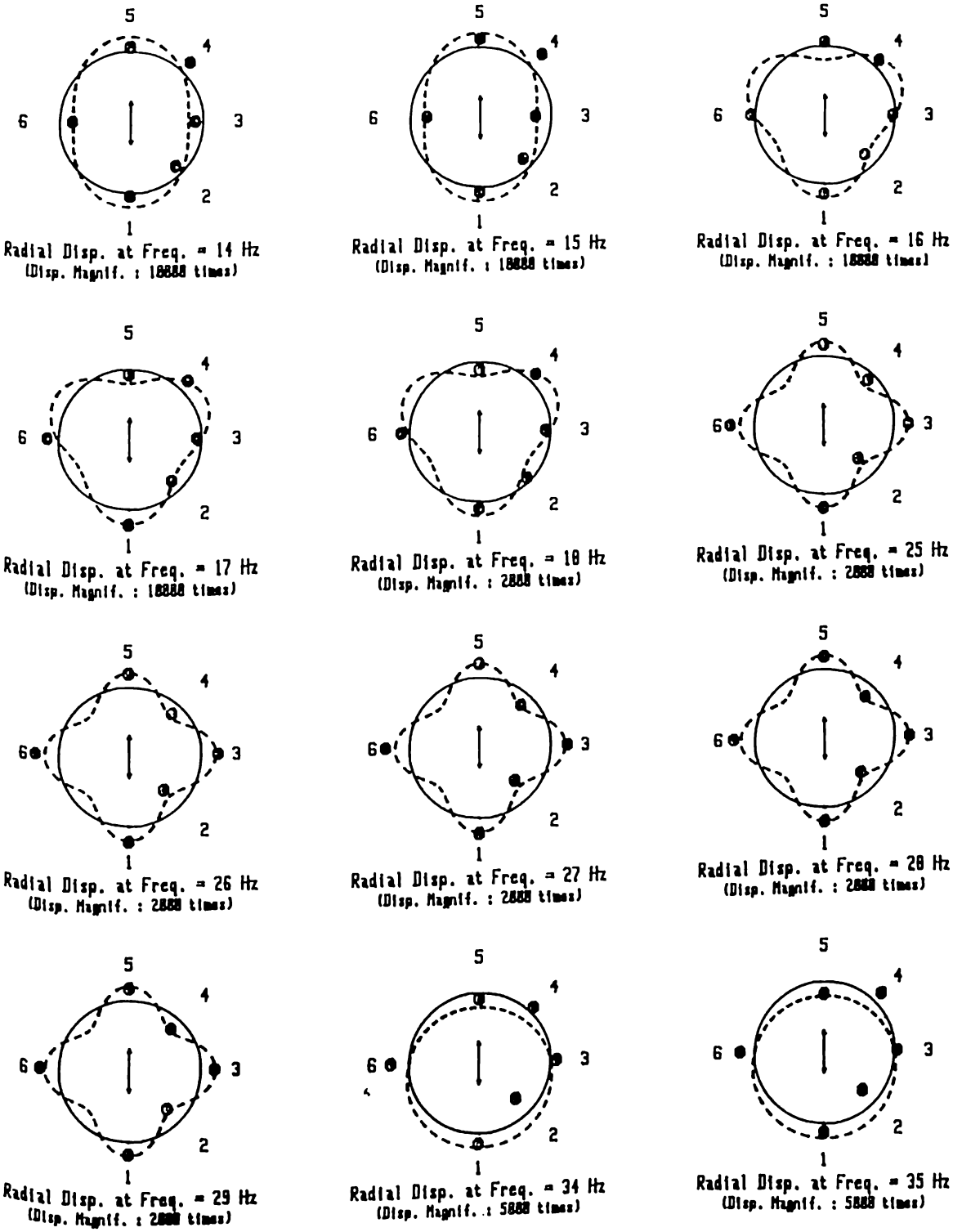

Fig. 9 - Experimentally obtained circumferential mode shapes

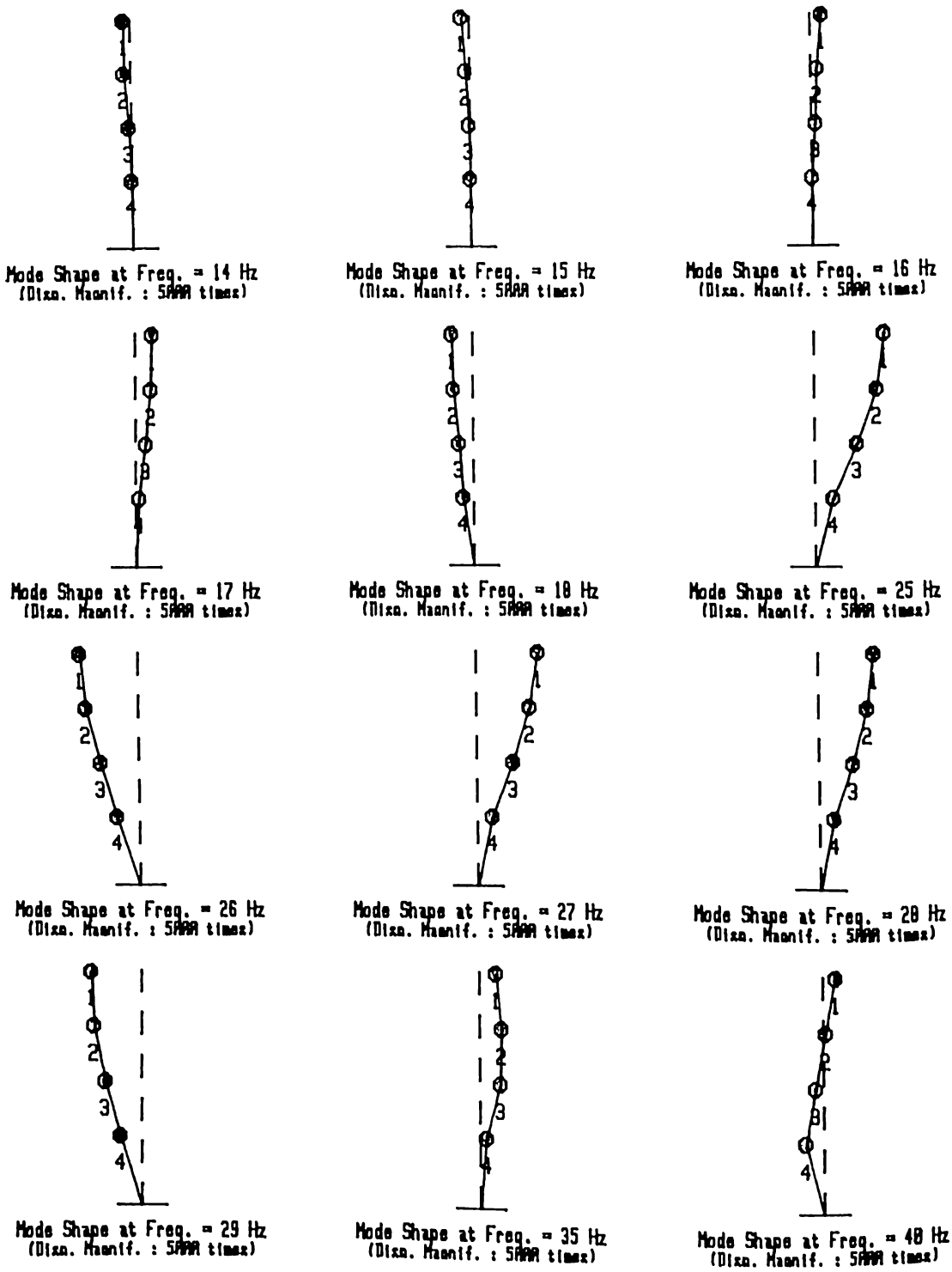

Fig. 10 - Experimentally obtained longitudinal mode shapes

The initial displacement was released by cutting the string with a scissor. The sensors used to monitor the vibration were the 6 strain gages measuring the circumferential strains and a displacement transducer measuring the displacement at the top of the model at $\theta = 180^{o}$. Vibration was monitored and recorded for a period of 1.024 sec. starting from the time the initial displacement was released. The sampling interval was 1 millisecond. The time history response is given in Figure 11. Spectral analysis was performed and the results are presented in Figure 12. Peaks observed at 16.462 Hz, and 28.320 Hz matched those of the calculated natural frequencies for modes (m,n) = (1,2) and (1,4), respectively. It is noticed that the amplitude at 16.462 Hz is very much greater compared to that at 28.320 Hz indicating that the circumferential shape of n=2 dominated. The peak observed at 0.976 Hz is not considered as one of the natural frequencies. This is only brought about by strains being offset from zero as shown in the graph in Figure 11 for channels 1, 2, and 6. This offsetting phenomenon may be caused by overstretching of the strain gages near the string. Smaller initial displacement was tried to avoid this but the resulting strains and displacements were too small to be properly monitored. The free vibration test was repeated five times and the results were identical.

EVALUATION OF DAMPING

Damping was evaluated by measuring the decay of vibration. The model was given an initial steady-state vibration via the shaking table. Then the input signal was cut off to terminate the applied excitation. As soon as the signal was cut off, the vibration of the model was recorded. Shown in Figure 13 is the decay record of the model which was initially vibrating at 27 Hz. The measurement set-up was similar to that of the steady-state vibration test. The decay was monitored for 0.512 second starting from the time the input signal was cut off. The sampling interval used was 1 millisecond.

To calculate the damping from the decay record, it is assumed that the decay is exponential in function, that is

$$Yi = k\, e^{(-2 * \pi * h * i)}$$

where i is the cycle number, and Yi is the ordinate of the ith cycle. The damping factor, h, and the equation constant, k, were calculated using the least square method for curve fitting the exponential function. Presented in Table 5 are the measured damping factor at frequencies 25 Hz to 29 Hz.

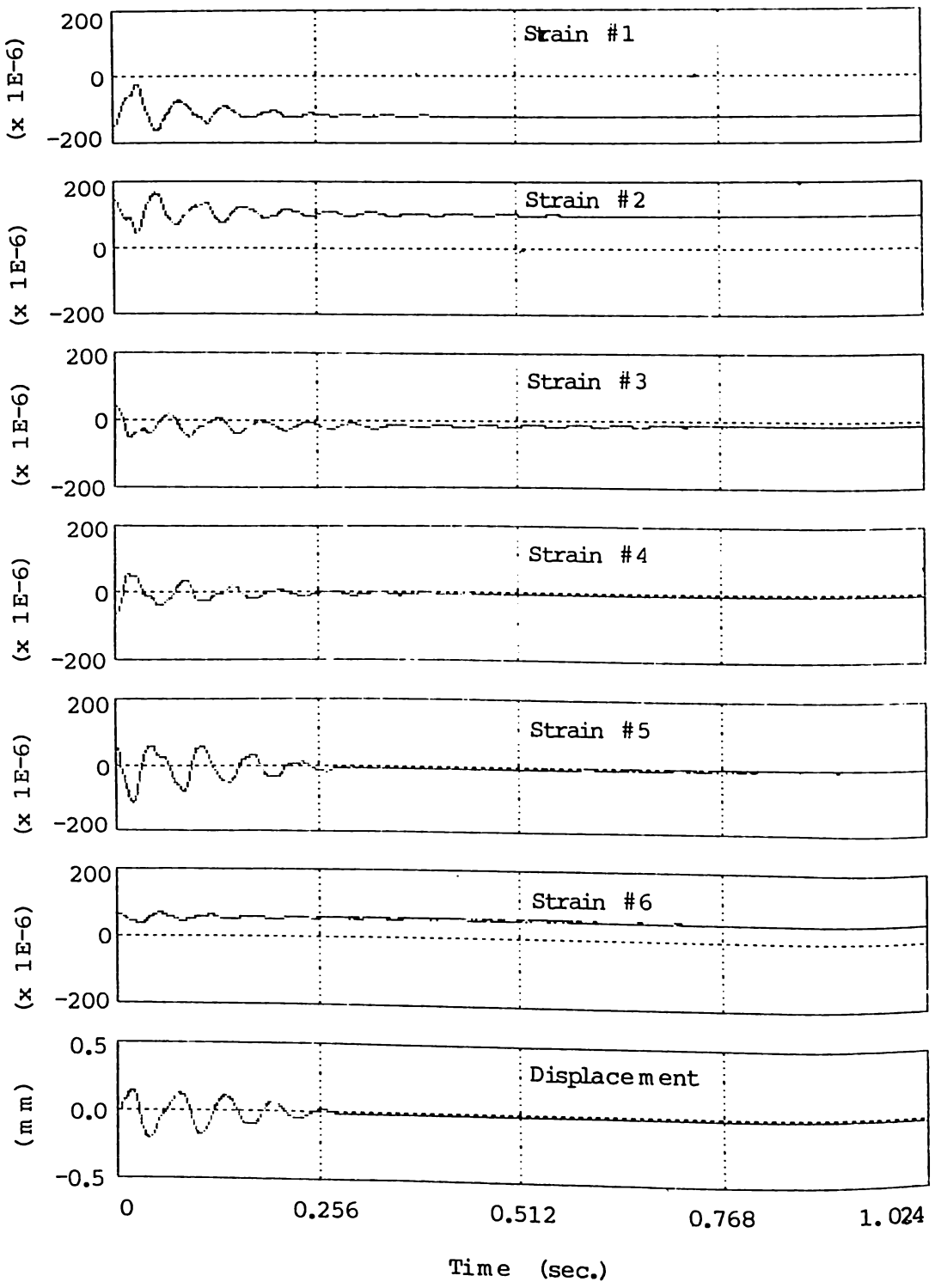

Fig. 11 - Time history record of free vibration

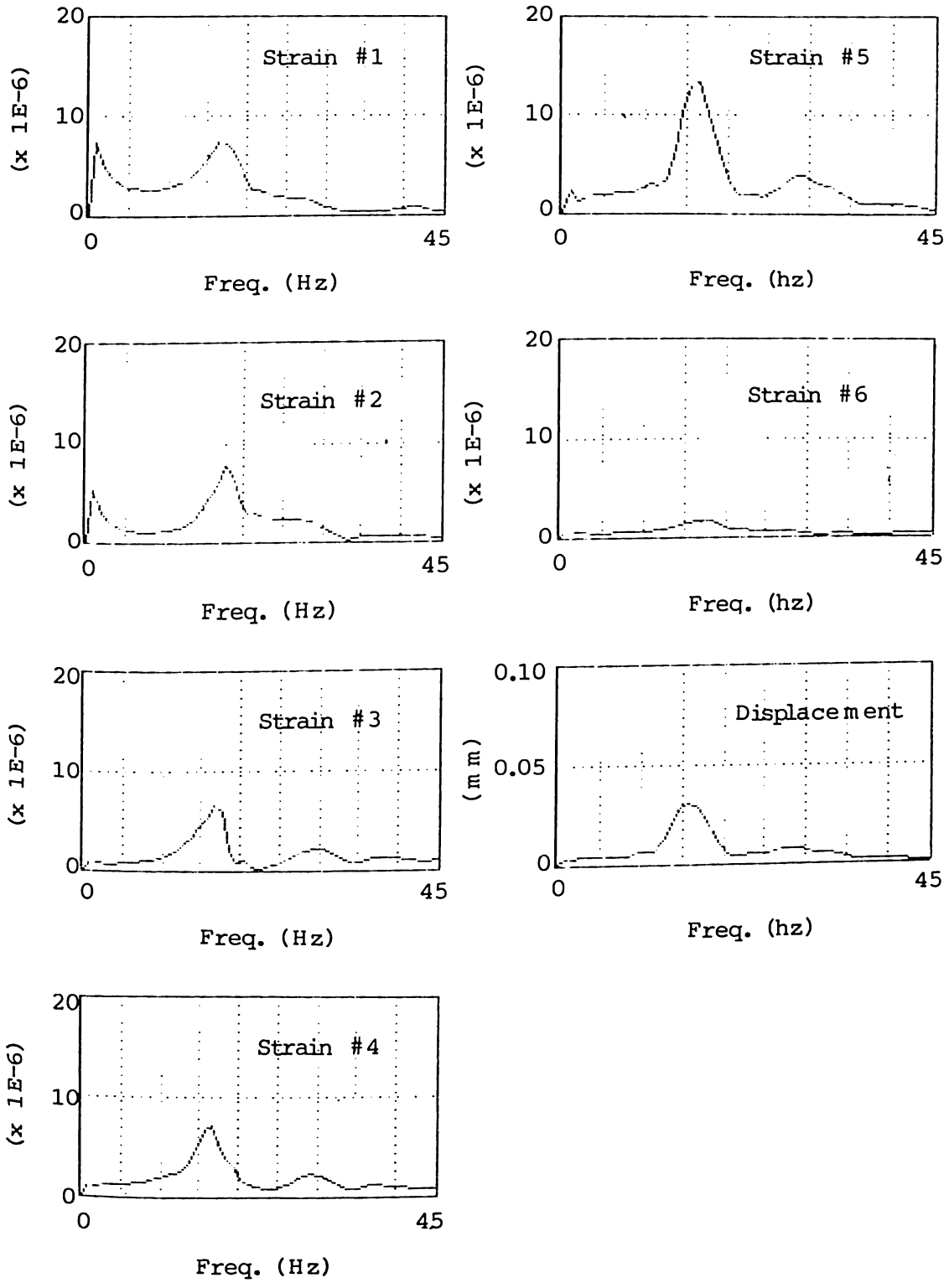

Fig. 12 - Spectra from free vibration test.

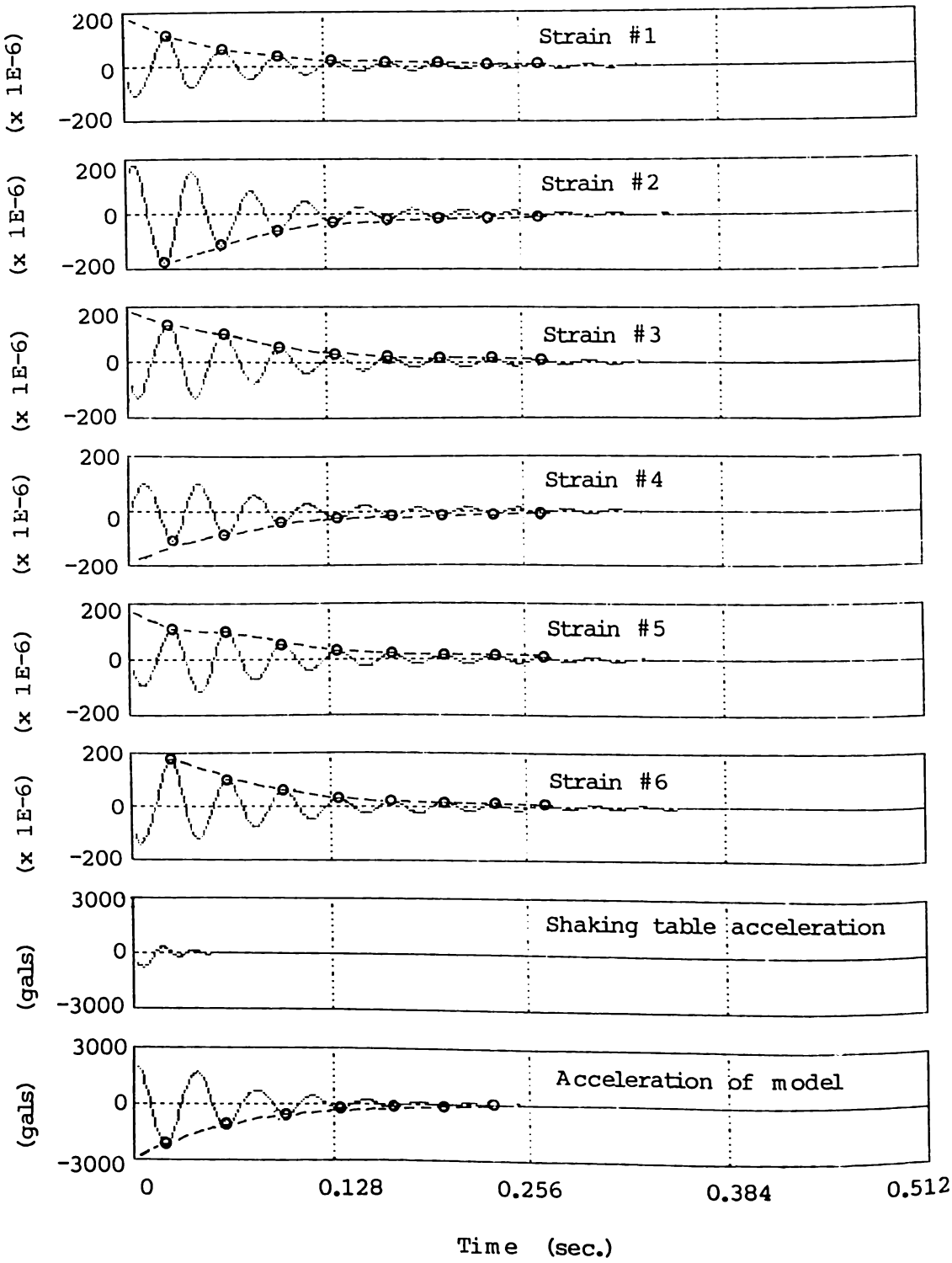

Fig. 13 - Decay record for evaluation of damping (previously vibrating at 27 Hz)

Table 5 - Summary of measured damping factor

Freq. (Hz)	Measured Damping Factor (h%) at the ff. sensors						
	#1	#2	#3	#4	#5	#6	#8
25	5.81	7.20	6.27	5.54	6.18	6.33	11.16
26	5.82	6.50	6.16	5.67	5.40	5.40	8.90
27	5.70	6.96	6.23	5.54	5.85	6.48	10.52
28	4.55	5.70	5.29	4.55	5.55	5.60	12.96
29	4.32	4.94	5.03	4.33	5.08	5.08	7.92

These initial vibration frequencies were chosen because they are near the experimentally obtained natural frequency corresponding mode (m,n) = (1,4). It was also attempted to measure damping at the other experimentally obtained modes, however, the resulting decay records showed non-uniform repetition of cycles such that the presented method for calculating damping cannot be used. However, it is hypothesized that the value of damping factor for the other modes are within the proximity of that obtained for mode (m,n) = (1,4).

It is noted that the damping factor measured using the acceleration meter is higher than the damping factor measured using the strain gages. The reason may be due to the difference in sensitivity of the two sensors. However, this is not critical since the damping factor obtained are not big enough to cause considerable change in the values of the natural frequencies. The relation between damped and undamped natural frequency is

$$\omega_d = \omega\sqrt{1 - h^2}$$

where ϖ_d is the damped natural frequency while ϖ is the undamped natural frequency. Therefore, damping factor of the range 5% to 10% will produce only 0.12% to 0.50% change in the natural frequencies which are practically negligible.

REMARKS ON EXPERIMENT RESULTS

Three tests were performed to determine experimentally the natural frequencies of the model. A summary of the natural frequencies obtained from these 3 tests is presented below.

Table 6 - Summary of natural frequency obtained from experiment.

Type of Test	Frequency (Hertz)		
	n=2	n=3	n=4
Frequency Sweeper	15.342	18.309	26.683
Steady-state	14	18	26
Free Vibration	16.462	--	28.320
FEM (calculated)	16.579	17.112	28.961

A reasonable conformance between the test results and the calculated natural frequencies is obvious. The slight differences are tolerable and may be due to several factors, among them are geometrical imperfection, difference in sensitivity of measuring devices, imperfect seam connection, coupling of modes, damping, etc. It is observed that lower values were obtained from forced vibration test compared to those from free vibration test. This may have been caused by the different manner by which vibration was induced to the model. Another factor that may have caused this is the different manner by which sensors react to each test. The slightly higher values obtained from the frequency sweeper test over those from the steady-state vibration test may be due to the increasing inertia force (applied to the model during the frequency sweep) as the frequency was increased creating a fictitious higher amplitude barely after the true occurrence of resonance. Also, note that in the steady-state vibration test only whole-numbered frequencies were used such that exact occurrence of resonance may still be between these whole numbers.

In free vibration test, the two natural frequencies that were obtained showed very small difference compared to the calculated ones. The maximum deformation occurred at the lowest natural frequency which was expected. The mode (m,n) = (1,3) was not obtained because its signal may have been very weak due to early decay or it may have been overwhelmed by the effect of the nearest mode (m,n) = (1,2).

In forced vibration test the 3 lowest natural frequencies corresponding to modes (m,n) = (1,2), (1,3), and (1,4) were distinctly excited with mode (m,n) = (1,4) exhibiting maximum deformation. It is surmised that mode (m,n) = (1,1) had been excited also since the amplitude at this frequency (at around 35 Hz) is considerably large and comparable in magnitude to that of mode (m,n) = (1,2) and (1,3). However there is no distinct peak in the spectra to clearly identify this mode.

Theoretically, a cylindrical shell with a fully restrained base will allow only an n=1 Fourier series loading of inertial force to the model. The presence of components other than n=1 indicate a perfect n-1 loading was not properly simulated. One reason is that a fully

restrained condition may have not been attained. Another possible cause may be the presence of geometrical imperfections. These may have happened even though every precaution was meticulously observe to achieve a perfect simulation of a clamped-free cylinder. Another probable reason is a distorted interaction between the model, plyboard base, and the shaking table. As indicated by the result, the loading of inertial force to the model was more of the $n=4$ Fourier series component. This may also be one of the reasons why the natural frequencies obtained by forced vibration is slightly lower than those obtained by free vibration.

In general, the results of the 3 tests complimented each other and prove the authenticity of the numerically obtained dynamic characteristics of a cylindrical shell. Differences in results are small enough and can be attributed to unintentional mismatching between the mathematical model and the actual condition of the shell.

ACKNOWLEDGEMENT

This study was carried out as part of the research program conducted by the Civil Engineering Divison of the Integrated Research and Training Center at the Technological University of the Philippines. The expirement results are also part of a masteral thesis submitted by the author to the Graduate Division of the College of Engineering, University of the Philippines. The author expresses sincere gratitude to Dr. Salvador F. Reyes of the Department of Civil Engineering, University of the Philippines for his technical advice.

REFERENCES

1. Bathe, K.J., Finite Element Procedures in Engineering Analysis, Prentice-Hall, New Jersey, 1982.

2. Baxter, B.D, Beckman, J.J., and Brown, H.A., Measurement Technique, Shock and Vibration Handbook Vol.1, McGraw-Hill Book Co., New York.

3. Leissa, A.W., Vibration of Shells, NASA SP-228 Washington D.C., 1973.

4. Lejano, B.A., Finite Element Method and Experimental Investigation of the Dynamic Characteristics of Vertical Cylindrical Shell, MSCE thesis, University of the Philippines, September, 1989.

5. Lunney, E.J., Introduction to Data Analysis and Testing, Shock and Vibration Handbook Vol.2, McGraw-Hill Book Co., New York.

6. Onate, E. and Suarez, B., A Unified Approach of Bridges, Plates and Axisymmetric Shells Using The Linear Mindlin Strip Element, Computers and Structures, v.17, no.3, 1983, pp. 407-426.

7. Sharma, C.B. and Johns, D.J., Natural Frequencies and Clamped Free Circular Cylindrical Shells, Journal of Sound and Vibration, v.21, no.3, 1972, pp.317-327.